Limnol. Oceanogr., 57(2), 2012, 582–596

doi:10.4319/lo.2012.57.2.0582

Coastal fronts set recruitment and connectivity patterns across multiple taxa

C. B. Woodson,[a,b,*] M. A. McManus,[c] J. A. Tyburczy,[d] J. A. Barth,[e] L. Washburn,[f] J. E. Caselle,[g] M. H. Carr,[h] D. P. Malone,[h] P. T. Raimondi,[h] B. A. Menge,[d] and S. R. Palumbi[i]

[a] Environmental Fluid Mechanics Laboratory, Stanford University, Stanford, California
[b] Center for Ocean Solutions, Stanford University, Monterey, California
[c] Department of Oceanography, University of Hawai'i at Manoa, Honolulu, Hawaii
[d] Department of Zoology, Oregon State University, Corvallis, Oregon
[e] College of Oceanic and Atmospheric Sciences, Oregon State University, Corvallis, Oregon
[f] Geography Department, University of California, Santa Barbara, California
[g] Marine Science Institute, University of California, Santa Barbara, California
[h] Ecology and Evolutionary Biology, University of California, Santa Cruz, California
[i] Hopkins Marine Station, Stanford University, Pacific Grove, California

Abstract

We show that ocean fronts set recruitment patterns among both community-building invertebrates and commercially important fishes in nearshore intertidal and rocky reef habitats. Chlorophyll concentration and recruitment of several species of intertidal invertebrates (*Balanus* spp., *Chthamalus* spp., *Mytilus* spp.) and rockfishes (*Sebastes* spp.) are positively correlated with front probability along the coast of the California Current Large Marine Ecosystem. Abundances of recent settlers and adults for nearshore rockfish species are also positively correlated with front probability. The interaction of coastal topography and bathymetry sets spatial scales of fronts and consequently recruitment at approximately 50 km during active upwelling, compared to 200 km or greater during non-upwelling periods. Such relationships between fronts and recruitment are likely to be consistent across other marine ecosystems—from coastal waters to the open ocean—and provide a critical link between adults and widely dispersing young. Ocean fronts, already known as features with high biodiversity and resilience in pelagic habitats, also set recruitment and connectivity patterns across multiple taxa for intertidal and rocky reef communities, thus linking biodiversity and resilience in coastal and benthic habitats as well.

Ocean fronts, boundaries between water masses characterized by gradients in ocean properties (e.g., temperature, salinity), are known as regions of increased abundance and diversity of taxa ranging from phytoplankton through most intermediate trophic levels to apex predators including humans (Wolanski and Hamner 1988; Ainley et al. 2009; Belkin et al. 2009). These ocean features often persist near shelf breaks and river mouths and at abrupt changes in coastline or bathymetry such as seamounts (Genin 2004). Fronts also may accumulate dispersing young because of a combination of convergent flow and organism behavior (Roughgarden et al. 1991; Wing et al. 1995; Woodson and Mcmanus 2007), or act as barriers to transport (Mcculloch and Shanks 2003; Shanks et al. 2003), depending on spatiotemporal patterns of frontal development and persistence relative to adult habitats and larval behaviors. Thus, there is a potential for fronts to have large effects on recruitment and connectivity, the transfer of individuals or genetic material between populations. Consequently, fronts may also have strong effects on the sustainability and resilience of coastal marine ecosystems. Yet, the influence of fronts on recruitment variability has not been previously addressed at the large spatial (hundreds of kilometers) and temporal (months to years) scales relevant to current marine conservation efforts and fisheries management (Moffitt et al. 2011).

* Corresponding author: bwoodson@stanford.edu

In Eastern Boundary Current ecosystems, wind-driven upwelling brings nutrient-rich water to the surface along the coast seasonally. Fronts develop between the cold waters near the coast and the warmer offshore waters. The relaxation of winds can bring upwelling fronts to shore periodically, a process that has previously been linked to intertidal invertebrate recruitment (Roughgarden et al. 1991). Similarly, recruitment of crabs (*Cancer* spp.) and sea urchins (*Strongylocentrotus* spp.) has been attributed to poleward propagation of thermal fronts associated with warm-water lenses inshore of upwelling centers (termed "retention zones") during wind relaxations (Wing et al. 1995). In addition, rockfish juvenile abundances have been shown to be associated with oceanographic gradients such as fronts (Bjorkstedt et al. 2002; Landaeta and Castro 2006), although recruitment patterns have not been evaluated. At local scales, propagating fronts associated with internal tidal bores can aggregate larvae and lead to distinct recruitment pulses (Pineda 1999). In contrast, fronts may also act as barriers to cross-shelf transport, as has been shown for mussels and barnacles on the Oregon coast (Mcculloch and Shanks 2003; Shanks et al. 2003).

The lowering of coastal sea level associated with upwelling in Eastern Boundary Current systems leads to strong equatorward, along-shelf currents, which can separate from the coast in areas with rapid changes in bathymetry or coastline orientation, leading to separation of the along-shelf flow from the coast and development of persistent fronts (Graham and Largier 1997). Fronts can also be associated with stagnation points where two

oppositely directed flows meet, such as at a boundary between counter-rotating eddies, or where a flow encounters a coastal boundary or steep bathymetric feature (Genin 2004). Spatial variation in upwelling due to coastline variation consequently leads to alternating upwelling centers and retention zones (Graham and Largier 1997). Retention zones (or upwelling shadows) are regions between inshore upwelling fronts and the coast that are often located in bays or behind headlands. These zones have enhanced water mass residence time, have been linked to elevated larval abundances, and have been suggested as biological hotspots for highly advective upwelling systems (Mace and Morgan 2006; Morgan et al. 2011). Fronts also form between these coastally trapped, warm surface waters (retention zones) and cold, upwelled waters offshore (Graham and Largier 1997; Castelao et al. 2006). Such fronts are defined by enhanced temperature gradients and spatiotemporal persistence due to topographic control (Graham and Largier 1997; Castelao et al. 2006). However, variation in the wind field and the density of upwelled waters may influence the temporal appearance of the front and frontal stability. Such patterns in upwelling and fronts are common across the California Current Large Marine Ecosystem (CCLME) and in other upwelling systems.

For marine planktonic larvae, oceanographic conditions and processes are involved in almost all aspects of development and survival as well as transport to or from adult habitats. Fronts, where cold, nutrient-rich waters meet warmer waters that are better for growth, can provide optimal growing conditions for many phytoplankton taxa compared to surrounding waters (Traganza et al. 1987). Consequently, frontal regions often have increased food availability that can enhance larval development rate and survival (Brown and Roughgarden 1985). The aggregation of larvae through either passive accumulation or organism behavior near oceanographic gradients (e.g., fronts and clines; regions of enhanced spatial gradients in properties such as temperature, salinity, density, or nutrients) can thus increase survival and reduce dispersal significantly from hundreds to tens of kilometers (Woodson and McManus 2007).

Fronts have been linked to recruitment of several species across different spatial and temporal scales through specific process studies, yet the effects of persistent fronts on spatiotemporal patterns of recruitment and adult abundances over ecologically relevant time periods has not been directly evaluated. We address this gap using long-term records of front probability computed using satellite-derived sea surface temperature (SST), satellite-derived chlorophyll data, recruitment of intertidal invertebrates (barnacles, mussels) and nearshore rockfishes (*Sebastes* spp.), and adult rockfish abundance to test hypotheses regarding the influence of fronts on spatiotemporal patterns in recruitment across multiple taxa.

Barnacles of the genera *Balanus* and *Chthamalus* along with mussels of the genus *Mytilus* are the dominant filter-feeding invertebrates of the intertidal zone of the eastern Pacific (Strathmann 1985). *Balanus glandula* is a brooding species that releases live larvae from winter through late spring in California and in summer in Oregon with a pelagic larval duration (PLD) of 15–45 d. This barnacle shows stronger recruitment and higher abundances in the Oregon and northern California regions (Connolly et al. 2001). *Chthamalus* spp. barnacles also brood and spawn year-round; however, release of larvae is highest in the spring, and abundances peak in central and southern California. The PLD for *Chthamalus* spp. is from 14 to 21 d. *Mytilus* spp. release gametes into the plankton year-round in central and southern California and in the summer in Oregon, and larvae have a PLD of 9–21 d. *Mytilus* spp. show similar patterns of abundance to *B. glandula*, with higher abundances and recruitment at higher latitudes (Connolly et al. 2001; Broitman et al. 2008).

Rockfishes (*Sebastes* spp.) are common members of rocky reef communities across the eastern Pacific to depths of several hundred meters. The kelp–gopher–black and yellow–copper (KGB; *Sebastes atrovirens*, *Sebastes carnatus*, *Sebastes chrysomelas*, and *Sebastes caurinus*) complex is made up of nearshore bottom-associated species that inhabit kelp forests and rocky reefs to depths of 100 m (Caselle et al. 2010*a*). We include the copper rockfish in this group because, although it has been reported to settle earlier in the season than the KGBs, previous work has suggested that this species responds to oceanographic drivers in the same manner as the KGB group (Caselle et al. 2010*a*,*b*). This group typically begins releasing larvae between late April and early June. Pelagic juveniles spend 1–3 months in the plankton before recruiting to kelp canopy in July–August. The olive–yellowtail–black (OYB; *Sebastes serranoides*, *Sebastes flavidus*, and *Sebastes melanops,* respectively) complex is a mid-water group that releases young in March and April. Pelagic juveniles of this group spend 3–4 months in the plankton before recruiting to the kelp canopy between late May and late June. Blue rockfish (*Sebastes mystinus*) are also a mid-water species and have similar pelagic life history patterns to the OYBs.

We use 10+-year records of front probability, chlorophyll concentration, and settlement and recruitment records of these taxa along the eastern Pacific coast to test the hypotheses that (1) fronts set recruitment and adult abundance patterns across a large marine ecosystem; (2) this pattern is consistent across multiple taxa; and (3) the effects of fronts are consistent even in the presence of strong latitudinal gradients in both upwelling and recruitment.

Methods

Front probability—High-resolution SST images were obtained from the National Oceanic and Atmospheric Administration–National Marine Fisheries Service–Southwest Fisheries Science Center (NOAA–NMFS–SWFSC), Environmental Research Division, in Pacific Grove, California, through Ocean Imaging, Incorporated, and Oregon State University under funding from the National Science Foundation–Global Ocean Ecosystem Dynamics North Pacific Program. All images were processed to remove cloud cover using the histogram method (Cayula and Cornillon 1992), although cloud cover often matches SST and thus cannot be fully removed (Breaker et al. 2005). After cloud removal, monthly mean composites for the entire time record were calculated. These monthly composites were found to reduce

effective cloud cover to less than 5% compared to daily images (~ 10–95% cloud cover). Each monthly composite image was then filtered using a contextual, adaptive median filter (Belkin and Reilly 2009). The filter started with a 5 × 5-pixel window and determines if a pixel was a 1-dimensional minimum or maximum in the cardinal (north–south, east–west) and ordinal directions (northeast–southwest, northwest–southeast). If so, the pixel maintained the original value; if not, a 3 × 3-window median filter was applied. The window was increased until its variance plateaued or until it reached a window size of 15 × 15 pixels. If the coast was encountered, the window was sampled at the window size where the coast was first encountered and ignoring any data points on land. This technique allowed the filter to operate closer to the coastal boundary than a traditional median filter, which leaves a mask near the coast equal to the window size, and to enhance edges (fronts) in the SST image (Fig. 1a; Belkin and Reilly 2009).

The vector magnitude of the temperature gradient was then determined by calculating the E–W (dT/dx) and N–S (dT/dy) components separately and combined to give a gradient magnitude $\left[(dT/dx)^2+(dT/dy)^2\right]^{1/2}$. Statistical determination of front probability, P_f, was estimated by fitting a log-normal distribution (e.g., $P_f=(1/2\sigma_m\sqrt{2\pi})\exp\{-[(\ln x-\mu)^2]/2\sigma_m^2\}$ where $\mu_s=(1/n)\sum_1^n \ln x_i$ is the mean and $\sigma_m=(1/k)\sum_1^k\{[1/(n_k-1)]\sum_1^{n_k}(\ln x_{ik}-\mu_k)^2\}^{1/2}=.6061$ is the mean log-normalized standard deviation across the entire data set) to the probability distribution (normalized histogram) of the gradient magnitude using 1000 bins for each month of the record (Fig. 2a, df > 100,000, $R^2 > 0.9$ for all cases). We used the mean log-normalized standard deviation from the entire data set as a coefficient because we wanted to reduce the predictor to a single value, the mean temperature gradient, in order to use this method directly on monthly composite images. Replacing σ with σ_m resulted in less than 1% variation in estimates of P_f, and correlation coefficients were reduced by a maximum of 0.065. We also fit the data to both exponential and inverse Gaussian distributions. The log-normal distribution provided the best result. Further, the tails of the distributions were virtually identical between the exponential and log-normal forms (less than 0.1% variation). Next, the derivative of the log-normal curve was computed and the first point past the mode (bin with highest probability) where the rate of change dropped below the 90th percentile was determined (dashed line; Fig. 2a). This value was taken as the threshold in the front probability algorithm, x_t. This procedure allowed the threshold to vary for each SST image and account for stronger temperature gradients during summer months than during winter months. For each data point, a log-normal distribution was then computed using the monthly mean temperature gradient (μ_t) because for a single pixel location,

$$\mu_t=\frac{d}{dx}\left(\frac{1}{n}\sum_1^N T_{ijk}\right)=\frac{1}{n}\sum_1^N\frac{dT_{ijk}}{dx} \quad (1)$$

as an estimate of the temporal temperature gradient probability distribution at a single pixel over the month (Fig. 2b). The probability of front presence within a pixel, P_f, becomes the integral of $P(x > x_t)$ (Fig. 1b). In order to convert this value to the probability of front detection, P_f is multiplied by the probability of a good pixel (e.g., ratio of good pixels to total pixels). However, in our analysis, we used P_f directly and not probability of detection. This method saved significant computation time and performed reasonably well compared to the Canny edge detection method (Castelao et al. 2006) and the histogram method (Cayula and Cornillon 1992) on the shelf and better nearshore (i.e., within 5 km of the coast). Although this method cannot identify individual fronts, it can resolve spatiotemporal regions of high front activity over the longer sampling intervals (e.g., months and seasons) that are necessary to provide enough cloud-free data. Many of the upwelling fronts in the CCLME, as well as in other ecosystems, are topographically controlled and are particularly amenable to the probabilistic techniques employed here.

Errors were estimated from the offset from zero of the mode in the log-normal distribution of the gradient magnitude. When a front was not present, the typical situation, the gradient magnitude should be approximately zero. From this estimate, the error in the frontal probability was determined as the integral of the probability density function between zero and the value of the gradient at the mode divided by the number of observations.

To address spatial and temporal patterns in front activity, front probability was computed in 5 × 5-km bins for the coastline of the CCLME (362 bins; 1810 km) and autocorrelation functions were computed to estimate spatial parameters (size [the decorrelation length scale] and spacing [the distance between the decorrelation length scale and the next significant correlation] along the coast) for each month (temporal patterns).

Chlorophyll analysis—We obtained monthly SeaWIFs data for the entire study period at 5-km resolution. Chlorophyll data were then filtered and processed using the same methods used for front probability (Fig. 1c; Belkin and O'Reilly 2009). To evaluate if regions of elevated chlorophyll were correlated with front probability, we computed the correlation coefficient for all image pairs over the entire study region. Seasonal trends were removed by computing the monthly mean across a year and removing this canonical value from each month. Chlorophyll was positively correlated with front probability ($p < 0.05$ for all comparisons) across all months and years with correlations ranging from 0.08 to 0.51. Low values of correlation were most likely due to the lower resolution of the SeaWIFs data set used in this study (5-km grid) as opposed to the SST resolution (1.1-km grid). Filtering data to larger grids tends to obscure correlations between small-scale features that still are somewhat under-resolved by the 1.1-km SST resolution.

Invertebrate recruitment data—Recruitment data for barnacle *B. glandula*; barnacles *Chthamalus dalli* and *Chthamalus fissus* (hereafter *Chthamalus* spp.); and mussels

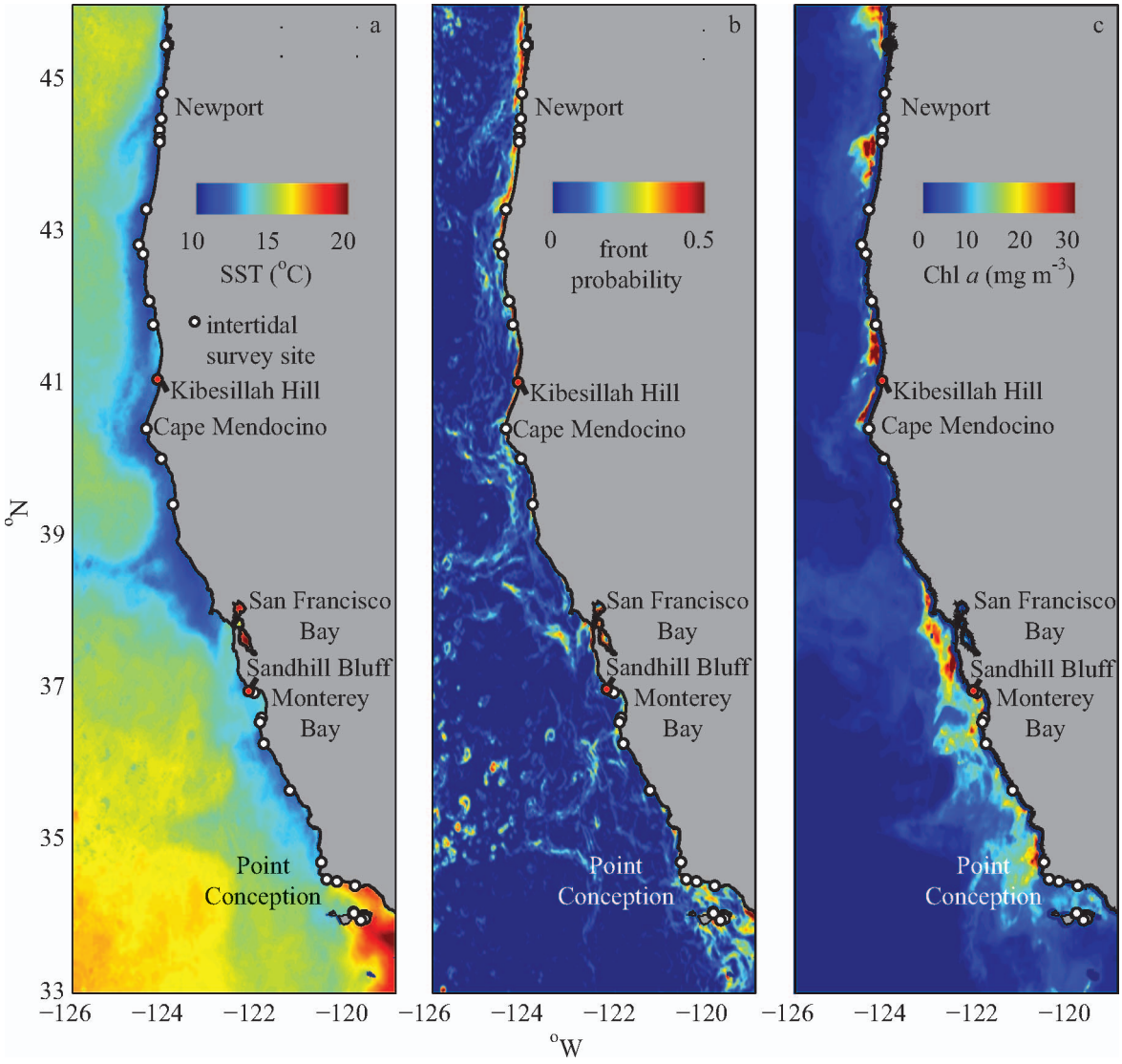

Fig. 1. (a) SST from Advanced Very High Resolution Radar (AVHRR) at 1.1-km resolution, (b) front probability, and (c) chlorophyll *a* (Chl *a*) concentration for the CCLME during June 2006 shown with intertidal sampling locations.

Mytilus californianus, Mytilus galloprovincialis, and *Mytilus trossulus* (hereafter *Mytilus* spp.) were obtained from the Partnership for Interdisciplinary Studies of Coastal Oceans (PISCO) long-term monitoring program and have been reported in a previous study by Broitman et al. (2008). PISCO measured recruitment at 31 sites across the CCLME (Fig. 1; *see* Web Appendix, Table A1, www.aslo.org/lo/toc/vol_57/issue_2/0582a1.html) using Tuffy (Clorox Inc.) scrub pads (mussels) and 10 × 10-cm polyvinyl chloride plates with Saf-T-Walk (3M Inc.) tape (barnacles) sampled approximately monthly (Broitman et al. 2008). Recruitment time series ranged from a minimum of 3 yr to a maximum of 7 yr. Each sample was collected and brought back to the lab for species identification and numeration by trained technicians. Data sets were then normalized to monthly values of daily recruitment rate (Broitman et al. 2008). We considered these samples "recruitment" because of the month-long integration of data that incorporates some amount of post-settlement mortality. It is important to note that Broitman et al. (2008) found high correlation between settlement (cyprids) and eventual recruitment (juveniles) for barnacles across many of the same sites.

In order to remove latitudinal gradients in invertebrate settlement, a linear, least-squares regression was performed between latitude and log-transformed recruitment (Fig. 3). Coefficients of the fits are given in Table 1. We then calculated the normalized recruitment, $\tilde{r}$, as

$$\tilde{r} = (r - \hat{r}) + \bar{r} \quad (2)$$

where $\hat{r}$ is the predicted value of recruitment from the latitudinal fit and $\bar{r}$ is the overall mean recruitment rate for the entire data set.

Rockfish abundance and recruitment data—Recruitment and settlement data for rockfish were obtained from the PISCO long-term monitoring program. For rockfish, we

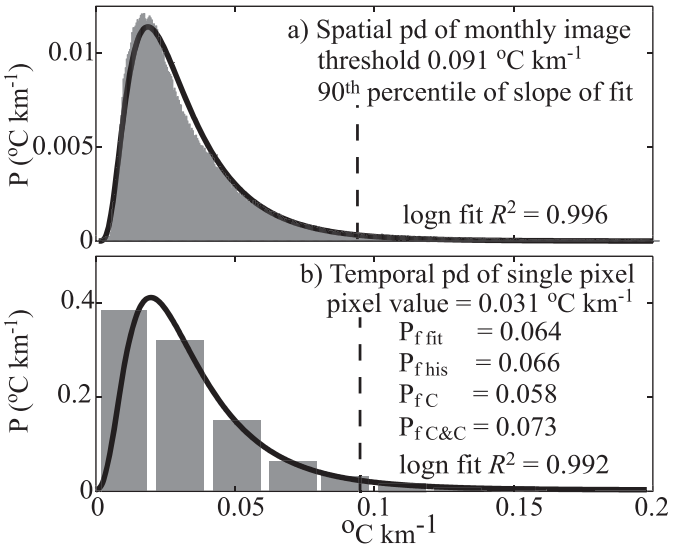

Fig. 2. Temperature gradient magnitude probability distributions (pd) over (a) full spatial domain for May 2004 (spatial pd), and (b) at a single pixel over all images within the month of May 2004 (temporal pd). Log-normal fit in (a) has μ_s = spatial average of temperature gradient magnitude over entire image, and in (b) μ_t = mean pixel value of the temperature gradient magnitude calculated from monthly image (in figure). R^2 values for all examined fits (> 500 pixels per month) were greater than 0.78. Dashed line is the location of the 90th percentile in the gradient used for front probability threshold. Front probabilities (P_f) in (b) are from the log-normal fit (*fit*), histogram (*his*), the Canny edge detection method (*C*), and the Cayula-Cornillon histogram method (*C & C*). Overall error between log-normal fits and histograms was 3.4% for all pixels examined over each month in the analysis (1999–2009).

identified "settlement" as arrival of pelagic juveniles into artificial collectors, and "recruitment" as young-of-year abundances from annual diver surveys, incorporating the typically high post-settlement mortality initially following settlement (Caselle et al 2010*a*,*b*). Recently recruited juvenile, young of year (YOY), and adult abundances were computed for two nearshore species complexes and one species (blue rockfish, *S. mystinus*). Nearshore YOY and adult abundances were measured from scuba surveys at 131 sites across central and southern California (Fig. 4; Web Appendix, Table A2). These surveys consisted of 30-m-long visual transects conducted at near bottom, mid water, and canopy. Settlement was monitored at a small subset (~ 20) of the sites (Fig. 4; Web Appendix, Table A2) in the Santa Barbara Channel and the Monterey Bay region. The rate of larval delivery (or settlement) to adult habitat for fishes was monitored using Standard Monitoring Units for Recruitment of Fishes (SMURFs). SMURF locations were sampled weekly or biweekly from May to November using a BINCKE net. Samples were hand sorted, visually identified to species complex, and stored for later analyses. A full description of the diver survey and settlement collector methods is available at http://www.piscoweb.org. Portions of this data set have been published previously by Caselle et al. (2010*a*,*b*).

Offshore pelagic juvenile abundances were taken from the NOAA–NMFS–SWFSC annual pelagic juvenile rockfish

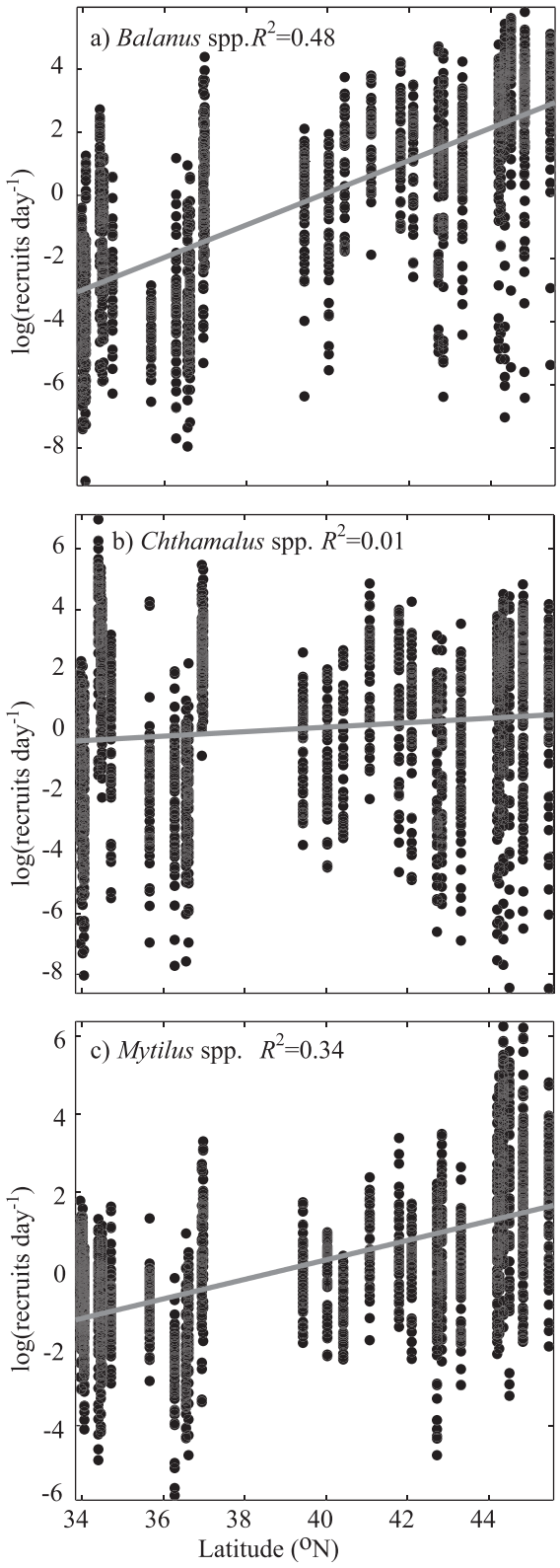

Fig. 3. Scatter plot of log-transformed recruitment data vs. latitude for (a) *Balanus* spp., (b) *Chthamalus* spp., and (c) *Mytilus* spp. Grey line is the linear fit ($\log(\hat{r}) = a(lat) + b$) used for normalization.

Table 1. Coefficients and R^2 values for regressions between latitude (lat), front probability (P_f), and log-transformed recruitment (r) for all three invertebrate species. PLD is in days. In equations, (r) is the daily recruitment rate; $\hat{r}$ is the expected value of recruitment from the latitudinal fit, and $\tilde{r}$ is the normalized recruitment anomaly after removal of the latitude (lat) regression. Numbers in parentheses are 95% confidence intervals. Coefficients reported only for significant regressions.

Species	PLD (d)	Lag (months)	Latitude fit ($\log(\hat{r})=a(\text{lat})+b$)			Front probability fit ($\log(\hat{r})=aP_f+b$)		
			a	b	R^2	a	b	R^2
Balanus spp.	15–45	0–2	0.51 (0.49, 0.54)	−20.34 (−21.33, −19.55)	0.49*	23.42 (21.98, 24.86)	−2.47 (−2.12, −2.82)	0.81*
Chthamalus spp.	14–21	0–1	—	—	0.01	19.66 (18.43, 20.87)	−2.23 (−1.65, −2.82)	0.88*
Mytilus spp.	9–21	0–1	0.25 (0.24, 0.27)	−9.76 (−10.35, −9.17)	0.34*	20.05 (14.27, 25.82)	−2.23 (−0.85, −2.44)	0.30*

* Significant at $\alpha = 0.05$.

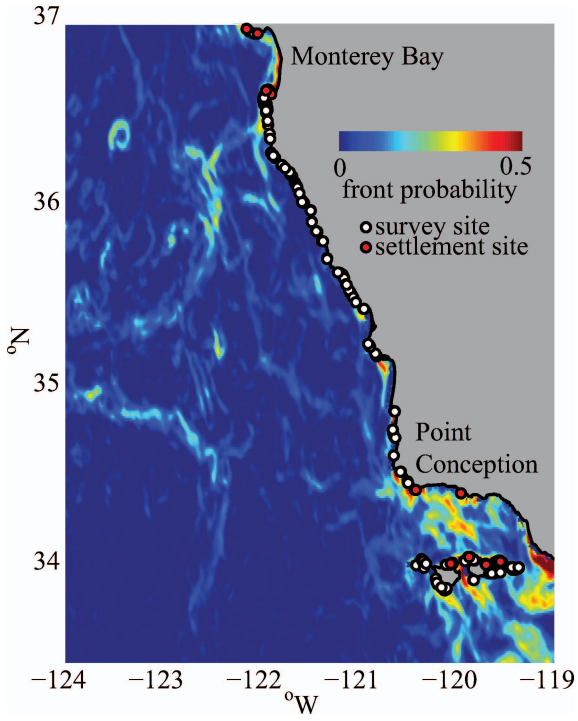

Fig. 4. Front probability for central and southern California during June 2006 shown with settlement (collector) and recruitment (diver surveys) sites.

cruises that have been conducted across California since 1986. This cruise has sampled established stations from Point Mendocino to southern California in May and June using a mid-water trawl (25-m depth). Abundances were computed as the annual mean from the entire cruise in each year. Although the nearshore species reported in this study are rare in these data sets, sample sizes were large enough to identify distinct patterns in interannual offshore abundances. We used taxonomic groups of rockfishes described in the introduction (KGB and OYB) for statistical analyses because (1) combined abundances provide higher statistical power, (2) it is virtually impossible to distinguish between all species within a group without genetic analyses, and (3) these groups are treated as units in nearshore fisheries (Caselle et al. 2010*a*).

Comparison of front probability and invertebrate recruitment—Mean front probability was computed for each site using a 5 × 5-pixel window perpendicular to the coast and centered at each location for specified lags of 0–2 months in order to cover the maximum PLD of all recruits for each group (Table 1). A neutral linear regression was then conducted between mean front probability over the period of larval dispersal (Table 1) and the log-transformed normalized recruitment, , because the normalized, untransformed data still did not meet normality assumptions. We used both annual means of front probability and recruitment as well as monthly data with seasonal trends removed to address potential spurious correlations related to seasonality. Monthly and annual means showed similar correlations with front probability, suggesting that seasonality did not significantly affect our results.

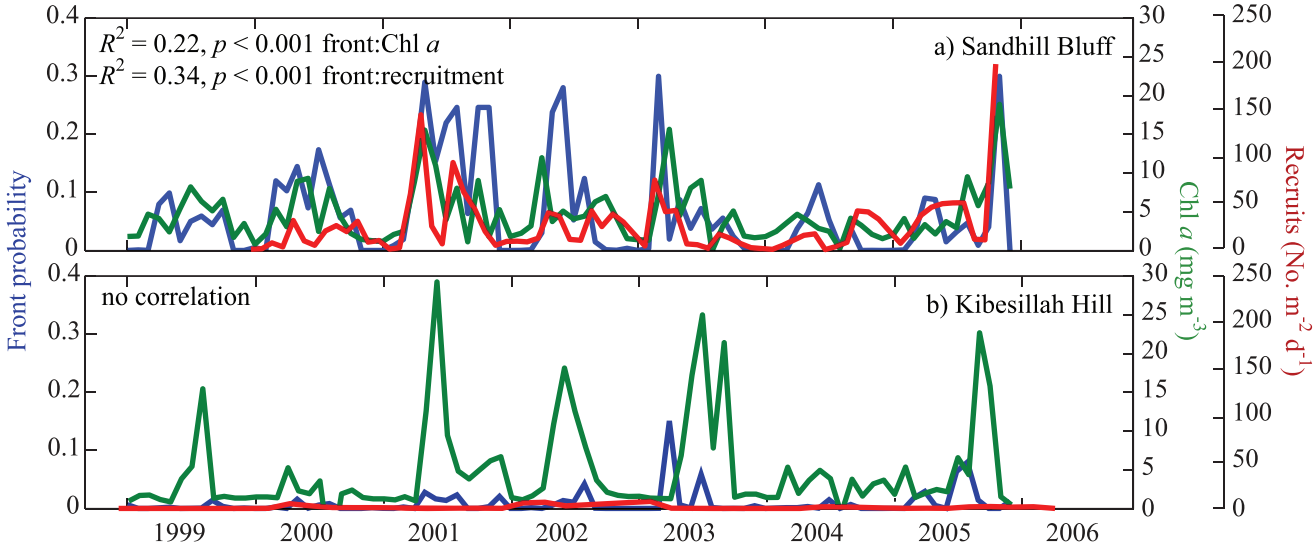

Fig. 5. Time series of monthly front probability, chlorophyll *a*, and recruitment of *Chthamalus* spp. (barnacle) at (a) high (SHB) and (b) low (Kibesillah Hill) front sites for 1999–2006.

We used the Kolmogorov-Smirnov test to evaluate the normality of the residual sum of squares (*RSS*) for all models. Residual independence was evaluated using temporal autocorrelation at each site. All residuals met these criteria for normality and independence. Because the latitudinal normalization constitutes an additional parameter in the invertebrate data sets, we combined the models and evaluated model performance using the Akaike Information Criterion (*AIC*; Akaike 1974):

$$AIC = 2k + n[\ln(RSS/n)] \quad (5)$$

where k is the number of model parameters (1 or 2), n is the sample size, and *RSS* is the residual sum of squares. For normally distributed, independent residuals, the *AIC* can be estimated with a correction for small sample sizes as

$$AIC_{R^2} = 2k + n\ln[(1-R^2)/n)] + 2k(k+1)/(n-k-1) \quad (6)$$

where R^2 is the "variance explained" or goodness-of-fit measure. Absolute values of the *AIC* are not informative, only the relative values where the lowest value is the model of choice.

Comparison of front probability and rockfish—Pelagic juvenile rockfish abundance from trawl surveys (Baltz 2009), settlement collectors (SMURFs) and diver surveys (YOYs) were totaled to get annual abundances across the entire sampling region. The pelagic juvenile rockfish cruises sampled offshore pelagic juvenile abundance and the diver surveys sampled nearshore YOY abundances over the same region of coastline. To address the effects of El Niño–Southern Oscillation (ENSO) variability, the Multivariate ENSO Index (MEI) was averaged over the maximum PLD for each species or complex (e.g., either 3 or 4 months). Then abundances from each year were categorized as warm (MEI $\geq$ 0.5, representing El Niño years) or neutral–cool (MEI $<$ 0.5, representing both La Niña and neutral years) based on the mean MEI over the maximum PLD. We used a threshold MEI value of 0.5 because all three rockfish groups in this study exhibit "normal" recruitment (defined as within one standard deviation of the log-transformed data) during La Niña (cool) and neutral conditions, and very low recruitment during anomalous El Niño (warm) conditions. Differences in recruitment between ENSO conditions were evaluated using a single-factor analysis of variance.

Fish recruitment did not display a latitudinal gradient, so fits were computed directly on the log-transformed data. Front probability was averaged over the PLD of each species or complex in the same manner as was computed for the invertebrate analysis with appropriate lags to match variability in the PLD (KGB, 0–3 months; OYB, 0–4 months; *S. mystinus*, 0–4 months). We again evaluated correlations between both monthly (with seasonal trends removed) and annual averaged data to address potential spurious correlations and found no effect of seasonality on our results. Thresholds of frontal effects were estimated using the ratio of the binned root mean square error (RMSE) to the total RMSE. Bins were computed at 0.025 intervals of front probability and then interpolated down to 0.01 increments for threshold determination as the peak in the rate of change in the probability density function. Temporal variability was analyzed by computing the coefficient of variation (C.V.) for all sites and bin averaging at 0.025 intervals of front probability.

Results

Intertidal invertebrates—Chlorophyll concentration and recruitment of *Chthamalus* spp. are temporally correlated at sites of comparatively high front activity such as Sandhill Bluff (SHB; Fig. 1) on the outer edge of the upwelling shadow in northern Monterey Bay (Fig 5a). In contrast, sites with comparatively low levels of front activity, such as Kibesillah Hill (Fig. 1), chlorophyll concentration and recruitment are not correlated with front probability (Fig. 5b). The sites shown in Fig. 5 are typical of patterns

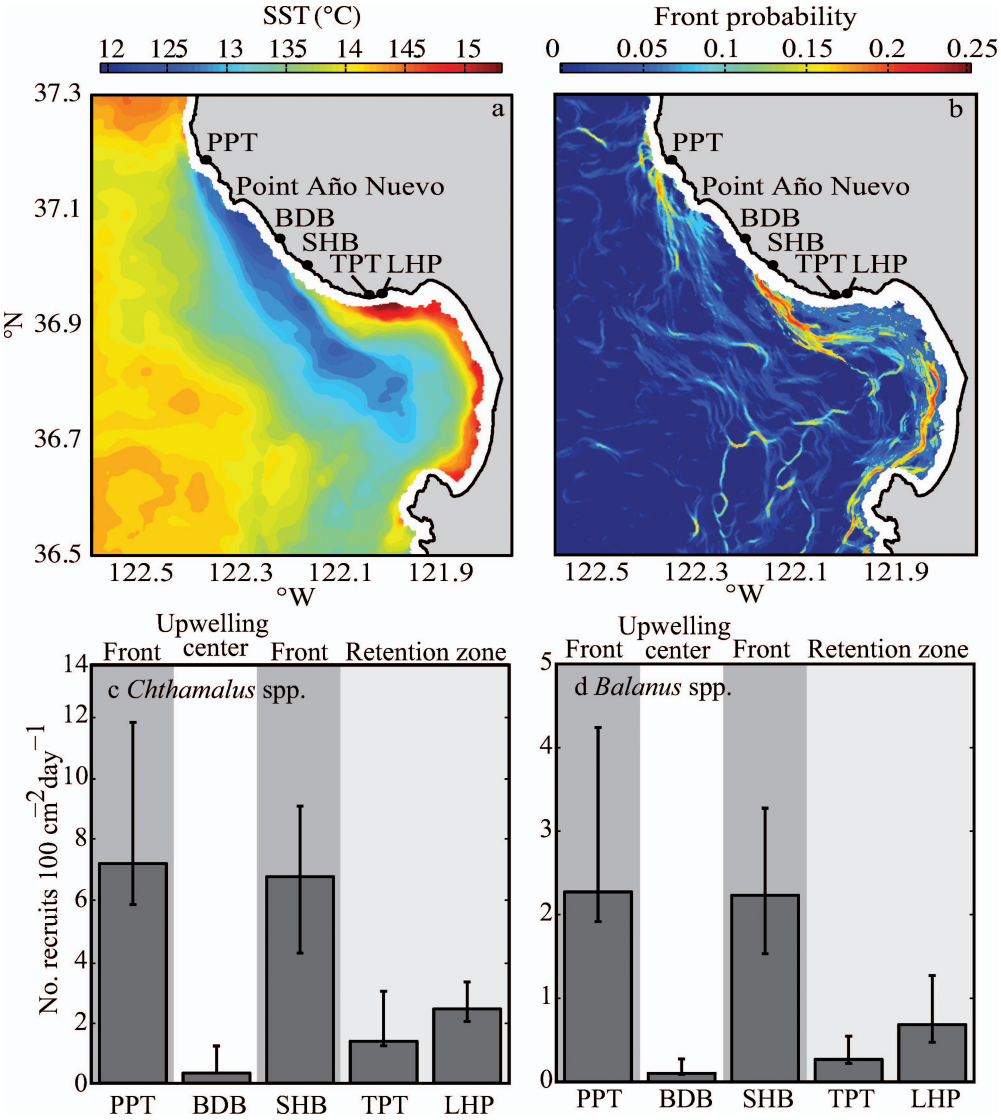

Fig. 6. (a) SST, (b) front probability, (c) *Chthamalus* spp. recruitment, and (d) *Balanus* spp. recruitment during upwelling season of 2007. (c,d) Error bars are 95% confidence intervals computed using bootstrapped resampling without replacement.

across the CCLME, with some sites exhibiting stronger correlations and some weaker.

In northern Monterey Bay, an upwelling jet originates at Point Año Nuevo and moves south across the mouth of the bay with fronts forming between cold, upwelled waters and warmer waters to the north, and within retention zones inshore of the upwelling jet (Fig. 6a,b; Graham and Largier 1997). We use the term "retention zone" here to define regions of enhanced residence time of waters in the lee of upwelling centers. This term, however, is not meant to imply retention of locally spawned larvae because larvae from any location may accumulate in these regions (Morgan et al. 2011).

Within the upwelling center (Bonny Doon Beach [BDB], characterized by $P_f < 0.10$, mean SST $< 12^{\circ}$C), recruitment is lower than in surrounding regions (Fig. 6c,d). Recruitment is highest in the regions of high front probability on either side of the upwelling jet (Pigeon Point [PPT] and SHB; characterized by $P_f > 0.10$). In regions away from the influence of upwelling and inshore of fronts, recruitment is intermediate (Terrace Point [TPT] and Lighthouse Point [LHP], characterized by $P_f < 0.10$, mean SST $> 12^{\circ}$C). Each of the sites reported here is characterized by rocky intertidal benches of similar geologic composition and intertidal communities dominated by mussels and barnacles, suggesting that substrate variability does not contribute to the observed patterns. At these relatively fine scales ($\sim$ 50 km), spatial patterns in recruitment of barnacles (*Chthamalus* spp., *Balanus* spp.) show that recruitment within retention zones (TPT, LHP) is elevated when compared to sites within regions of active upwelling (BDB; Fig. 6c,d; Morgan et al 2011). However, barnacle recruitment is significantly higher in regions of high front probability (SHB, PPT). This pattern is consistent across all years for PPT, SHB, and TPT. We show only 2007 here because BDB and LHP were only sampled as part of an intensive process study during this

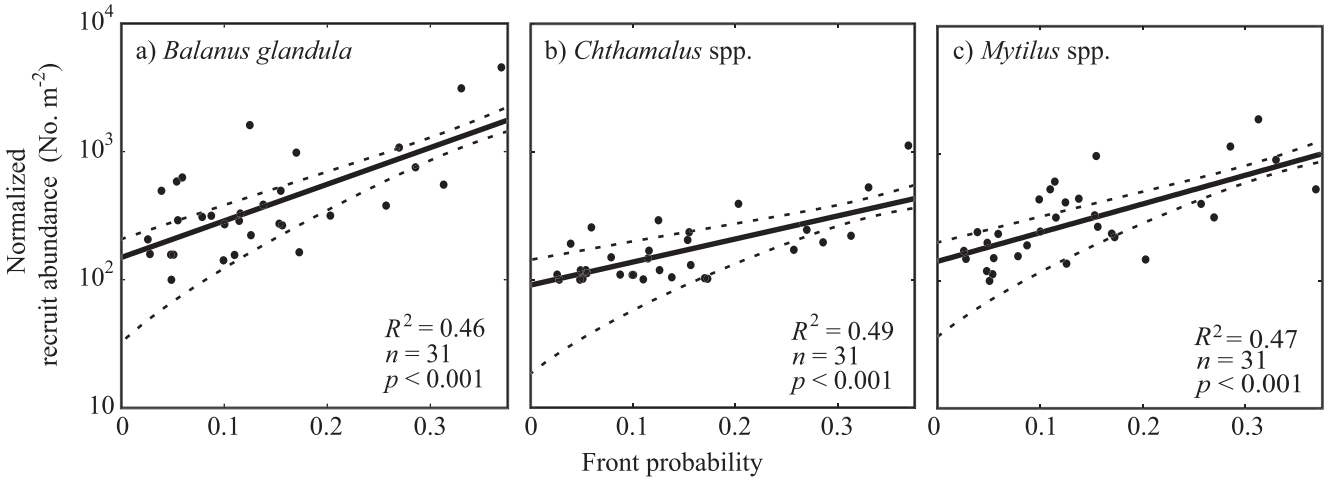

Fig. 7. Recruitment (monthly average over 8 yr of data, 1999–2006, for all 31 stations) and mean front probability within 5 × 5-km window centered on site location for (a) *Balanus glandula* (barnacle), (b) *Chthamalus* spp., and (c) *Mytilus* spp. (mussel) from 1999 to 2006. Dashed lines show 95% confidence intervals for fit.

year, although PPT, TPT, and SHB are part of the PISCO long-term sampling program.

Across the CCLME between 32°N and 46°N, recruitment is positively correlated with front activity for the two barnacle genera and one mussel across all stations and times sampled (Fig. 7). Based on the *AIC* where the lowest value represents the best model for a particular data set when employing multiple explanatory variables as described in Methods, the latitude-normalized front model performed better than other models for *Balanus* spp. and *Mytilus* spp., whereas the front-only model performed best for *Chthamalus* spp. (Table 2).

Rockfish settlement, recruitment, and abundances—Offshore abundance of pelagic juvenile rockfishes (*Sebastes* spp.) is not correlated with settlement for nearshore species (Fig. 8a). Offshore abundance and settlement of nearshore rockfish complexes appear to be inversely affected by variations in upwelling associated with ENSO. During El Niño (warm phases), there are high offshore abundances and low settlement, whereas during La Niña and in neutral years (cool phases), there are low offshore abundances and high settlement (Fig. 8b). Using an identical analysis to that used for invertebrates with front probability computed in a 5 × 5-km box centered on the sampling site, we find that settlement is correlated with front probability at several monitoring sites in central and southern California (Fig. 9a). The temporal C.V. in settlement decreased with increasing front probability (Fig. 9b; $R^2 > 0.5$ in all cases) suggesting that regions of high front activity experience not only higher overall settlement, but also lower variability in settler abundance.

Table 2. *AIC* for each model and genera from invertebrate analysis. Bold indicates best fit from *AIC* analysis.

	AIC		
Genera	Latitude-only model	Front-only model	Latitude+front model
Balanus spp.	−123	−99	**−153**
Chthamalus spp.	−105	**−162**	−154
Mytilus spp.	−115	−83	**−139**

We also found positive correlations between front probability and rockfish recruitment (YOY abundance; Fig. 10), suggesting that settlement of pelagic juveniles associated with fronts translates to spatial recruitment patterns. These correlations were not sensitive to the number of lagged months included in the computation for any species (or complex).

Correlation thresholds (χ) for the influence of front activity were computed based on root mean square values binned by front probability (Fig. 10). At low values of front probability, recruitment could be high or low, whereas at high frontal probability, recruitment was always high. The presence of a threshold suggests that fronts influence recruitment if they are relatively strong and persistent, but that other factors associated with transport and survival can also lead to high recruitment pulses. We found similar positive correlations between front probability and adult abundances for all species (Fig. 11), suggesting that high front activity regions are also biological hotspots across life stages, similar to results for intertidal invertebrates (Leslie et al. 2005). Adult abundance and front probability were not as strongly correlated, however, likely because of post-settlement movements of adults. We also found positive correlations between settlement and recruitment at sites where settlement collections and diver surveys coincided, similar to patterns observed by Broitman et al. (2008) for invertebrates.

Spatiotemporal patterns in front activity—Correlations between recruitment and front activity led to questions about how the spatiotemporal dynamics of these oceanographic features potentially shape connectivity patterns. We therefore computed the mean front probability across 5-km sections for the study region. A typical example of spatial patterns in coastal front probability during the upwelling season is illustrated in Fig. 12a. Using these data

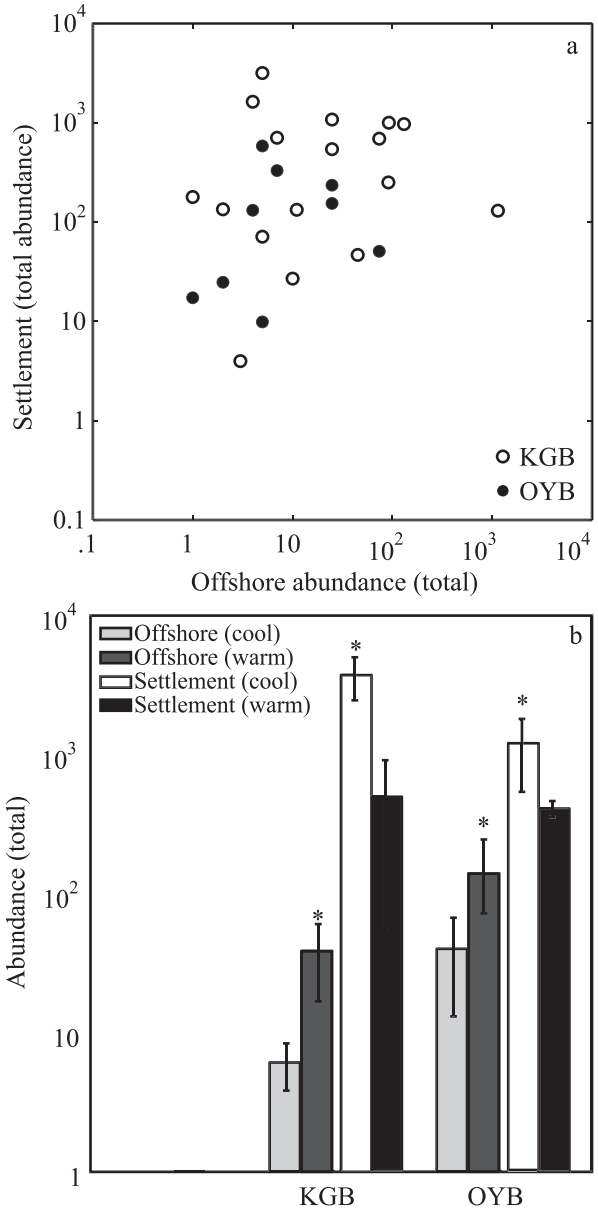

Fig. 8. (a) Offshore abundance of pelagic juvenile rockfishes sampled by trawl and settlement from 1999 to 2008 for two nearshore rockfish complexes (KGB [open circles] and OYB [filled circles]), and (b) mean annual abundance of pelagic juvenile rockfishes offshore and settlement separated by ENSO conditions. Error bars are the 95% confidence intervals. An asterisk indicates significant difference ($p < 0.05$) between ENSO categories.

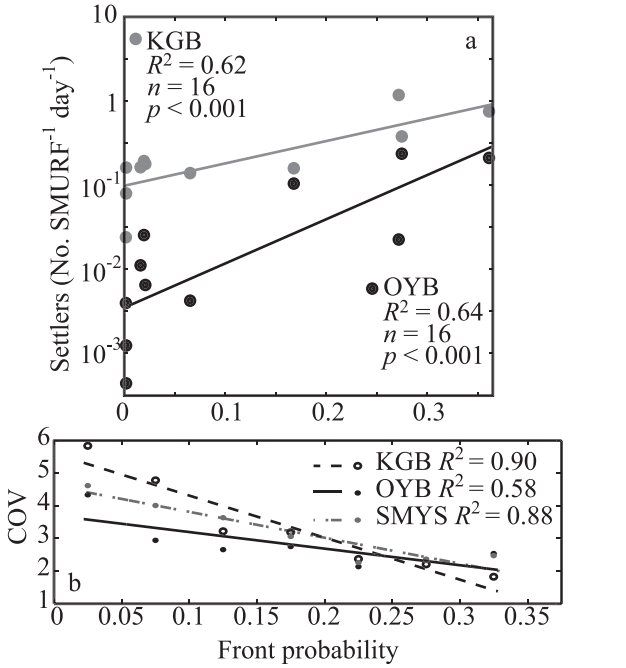

Fig. 9. (a) Settlement at site for KGB and OYB vs. mean front probability computed within 5 × 5-km window centered on site location, and (b) temporal coefficient of variation (COV) of settlement binned by front probability from sub-monthly recruitment data. SMYS, *Sebastes mystinus*.

across all months, we defined two parameters, size and spacing, based on characteristics of the autocorrelation functions. Size (the decorrelation length scale; Fig. 12b) represents the strength, persistence, and length scale of the frontal regions, and spacing (distance to first significant correlation beyond the decorrelation length scale; Fig. 12c) represents the distance between front regions. The size parameter was as high as 200 km in non-upwelling months (November–February), and was often less than 50 km during upwelling months (March–October; Fig. 12b). The space parameter was typically 150 km or more during non-upwelling months, and as small as 60 km during active upwelling (Fig. 12c).

These results suggest that during non-upwelling, fronts are large, weak, ephemeral, and far apart. Conversely, fronts during upwelling are strong, persistent, and close together. Because larvae are more likely to encounter persistent frontal regions close to release sites (simply because of proximity), fronts that are closer together and more persistent may in effect limit dispersal distances considerably.

In 2005, the CCLME experienced a 2-month delay in the onset of upwelling favorable winds and a crash in recruitment across multiple taxa (Barth et al. 2007). During this time, fronts remained weak, and far apart until upwelling commenced in May–June (Fig. 12b,c). The years 2004 and 2005 were the only outliers observed over the 10-yr record, and 2005 is shown separately because of its unique pattern of delayed upwelling, but it is included in the estimates of mean and confidence intervals.

Discussion

Front probability and recruitment are positively correlated for multiple taxa across the CCLME. Broitman et al. (2008), who addressed spatial recruitment patterns for the same invertebrate data set employed in this study, found that recruitment was positively yet weakly correlated with SST; however, they could not identify a specific mechanism for these patterns. Our results expand upon the findings of Broitman et al. (2008) by identifying fronts as a mechanism for enhanced recruitment that explains geographic

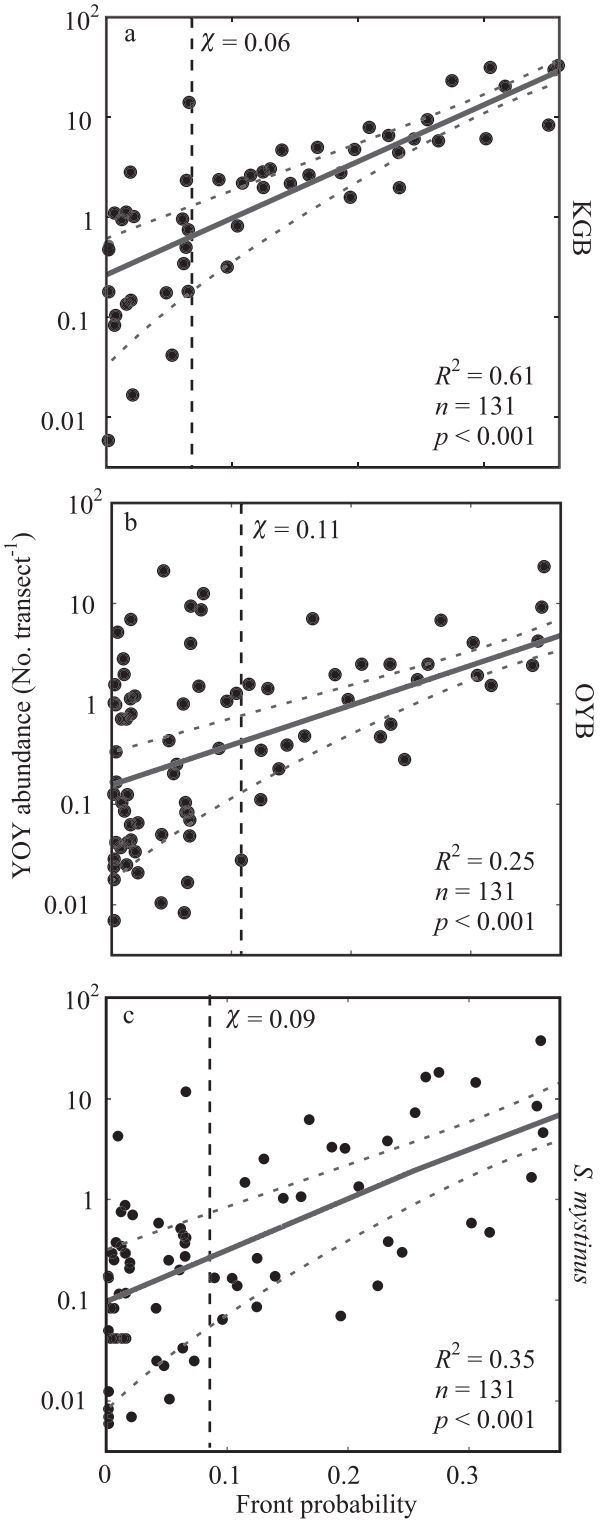

Fig. 10. Recruitment of rockfishes (YOY abundance) to adult habitats (kelp forests) estimated from diver surveys vs. mean front probability computed within 5 × 5-km window centered on site location for (a) KGB, (b) OYB, and (c) blue (*Sebastes mystinus*) rockfishes.

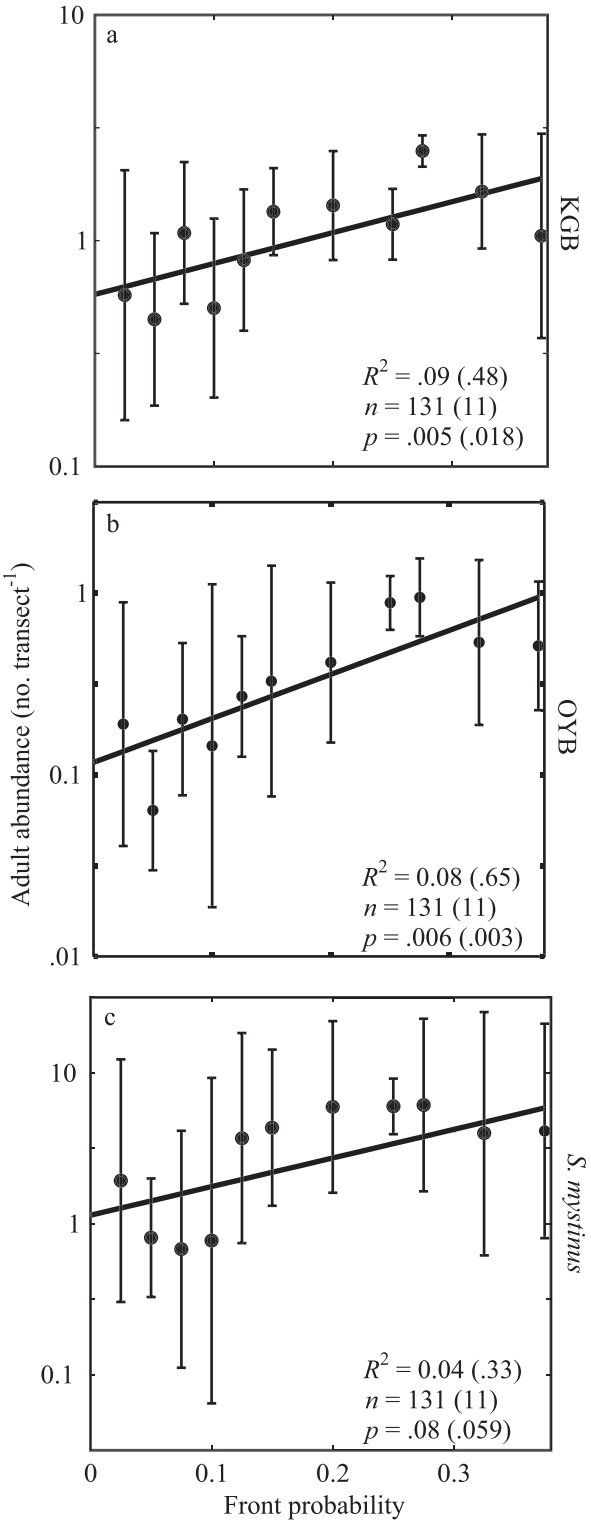

Fig. 11. Adult abundances of rockfishes estimated from diver surveys vs. annual monthly mean front probability computed within 5 × 5-km window centered on site location for (a) KGB, (b) OYB, and (c) blue rockfish (*Sebastes mystinus*). R^2 and p values are reported for entire data set and for sites binned by mean front probability in parentheses (bin size = 0.05).

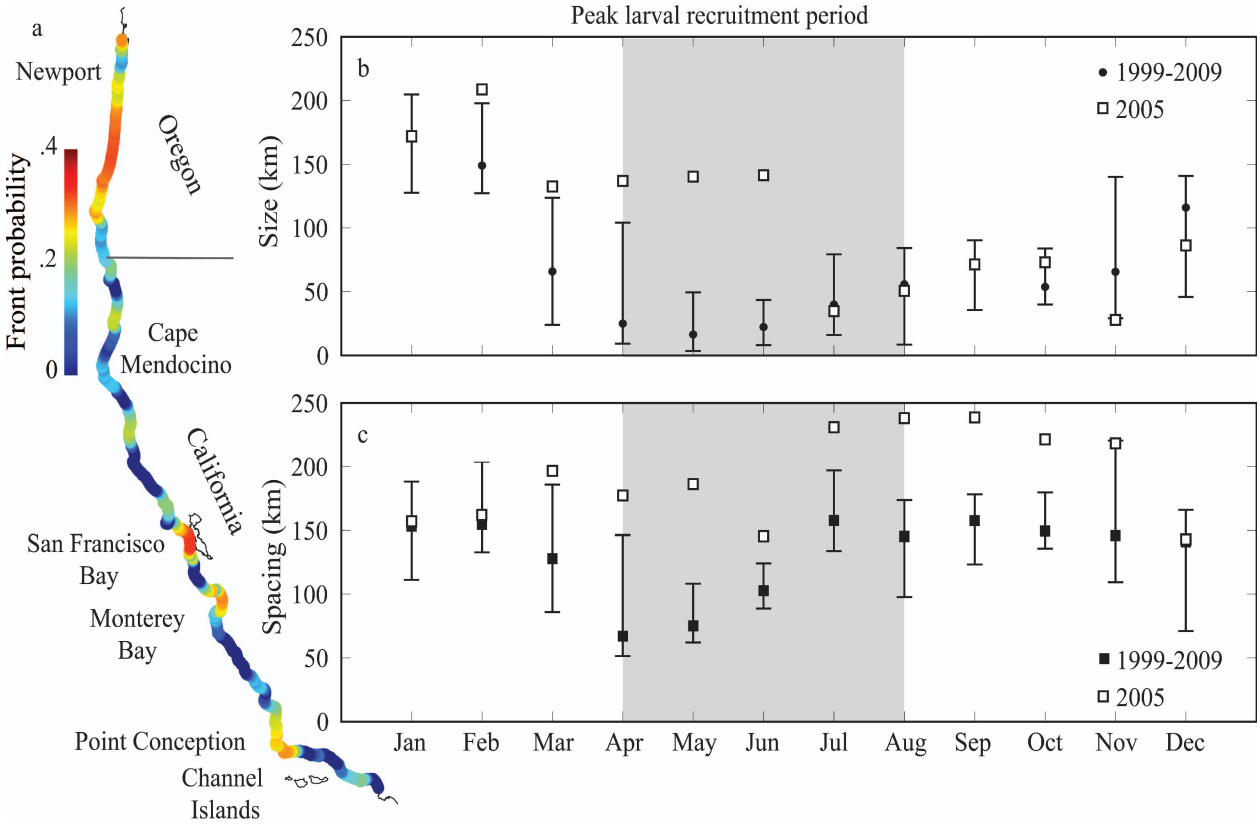

Fig. 12. (a) 5-km binned frontal probability along coast during June 2006. (b,c) Spatial structure of front probability averaged over 1999–2009 based on autocorrelation function (b, size—decorrelation scale; c, spacing—distance between decorrelation scale and next autocorrelation peak). Error bars show 95% confidence intervals. 2005 is shown separately as an example of the effects of delayed upwelling.

variability for all three invertebrate species, including the barnacle *Chthamalus*, which does not show a strong latitudinal gradient in recruitment. We found broad support for our hypotheses (1) that fronts set recruitment patterns across large spatial scales, (2) that this pattern is consistent across multiple taxa including both intertidal invertebrates and nearshore rockfishes, and finally (3) that these patterns are consistent despite environmental or latitudinal gradients in upwelling and organism abundance. Our results suggest that fronts are likely important to recruitment variability in other upwelling systems (Queiroga et al. 2005), as well as other regions with persistent fronts, regardless of the physical mechanism that generates them. Employing our analyses on existing data sets in other systems may provide unique insights into this hypothesis.

Persistent fronts likely set recruitment patterns through a variety of biophysical coupling mechanisms. First, fronts are regions of enhanced shear and high vertical velocities that consequently act as accumulators of passive, buoyant particles and weakly swimming organisms, in particular phytoplankton and small zooplankton including larvae (Wolanski and Hamner 1988; Morgan et al. 2011). Therefore, enhanced accumulation of larvae could lead to the observed patterns where fronts have a strong influence on recruitment for comparatively weak-swimming intertidal invertebrate larvae (Fig. 7). Increased phytoplankton and zooplankton biomass at frontal regions may also lead to increased development rates and shorter PLD for the larvae of many species (Brown and Roughgarden 1985). Thus, timing and strength of frontal development may lead to variation in dispersal distance due to changes in PLD.

In contrast to invertebrate patterns, rockfishes show distinct thresholds for the influence of fronts on recruitment (Fig. 10). It is expected that accumulation of larvae (or prey resources, thus increasing survival) at stronger convergent fronts is responsible for these patterns. Such accumulation could be due to passive transport or larval behavior. For active behavior to be an effective mechanism of enhanced recruitment, the front must persist long enough to be exploited and have cues that can be employed by individual larvae. For example, strong swimmers such as pelagic juvenile rockfishes are known to aggregate at oceanographic gradients (Bjorkstedt et al. 2002; Landaeta and Castro 2006; Woodson and Mcmanus 2007). The lack of a threshold in the invertebrate data suggests that passive accumulation may not explain the threshold pattern observed in the rockfish data. Similar patterns between settlement and recruitment with respect to front probability implies that post-settlement prey availability is not solely responsible either, but may contribute to the observed relationships. We therefore hypothesize that juvenile rockfish behavioral responses to prey distributions may lead to the threshold patterns observed. However, the present data cannot address the specific mechanisms that

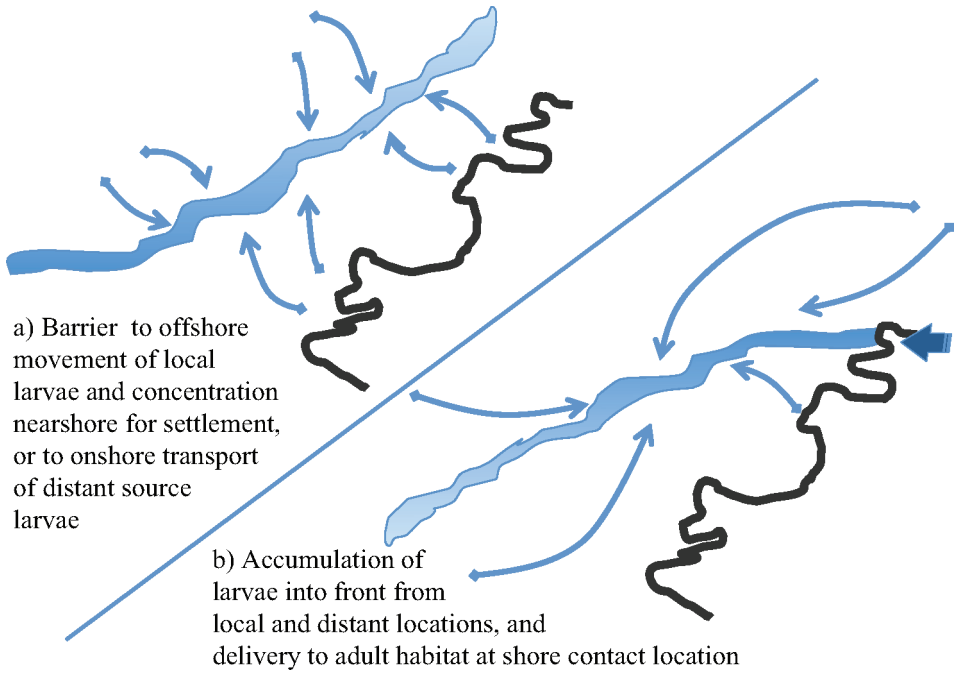

Fig. 13. Two ways ocean fronts can affect settlement, recruitment, and population connectivity. (a) The barrier model will decrease connectivity by fencing in local larvae and decreasing larval immigration. (b) The accumulation model will increase connectivity by gathering larvae from other locations and delivering these immigrants to shore. Most frontal features will operate along a spectrum between these two extremes and effects on connectivity could vary with different larval behaviors.

may lead to correlations between fronts and recruitment or to the presence of correlation thresholds.

Recruitment (i.e., density of YOY) of rockfishes was highly variable in regions with low front probabilities, suggesting that other mechanisms can also lead to high recruitment (Fig. 10). Regions with low front probability appear to be dependent on stochastic delivery of young by intermittent mesoscale processes (Mitarai et al. 2008). Because recruitment of larvae is a key component of resilience in marine ecosystems, regions of high front activity, where recruitment is less variable and generally higher, will be more resilient and sustainable compared to regions with low front probability. For example, a steady supply of foundation species, intermediate trophic levels (zooplankton and invertebrate larvae), and top predators (fishes) points to highly resilient communities that will recover quickly from both natural and man-made catastrophic events such as hurricanes, oil spills, and overfishing.

Interestingly, the pelagic larval period and peak recruitment for most of the species in this study is during the upwelling season along the northeastern Pacific Ocean. During upwelling, fronts are typically stronger and closer together (Fig. 12b,c), which may also explain patterns of adult abundance for intertidal invertebrates, where limited dispersal alone can be responsible for observed distributions in the absence of environmental variability (Gouhier et al. 2010).

Throughout 2004, because of weak upwelling, and in early 2005, because of a 2-month delay in the onset of upwelling favorable winds, fronts were weak and scales remained large in the spring and summer (Fig. 12b,c). The result of this pattern in upwelling was a decrease in recruitment for invertebrates (barnacles and mussels) and rockfishes, as well as the collapse of many seabird populations (Pierce et al. 2006; Barth et al. 2007). Delays in the onset of seasonal upwelling are a potential effect of climate change on coastal upwelling regions (Barth et al. 2007). When trying to understand how marine ecosystems will respond to future climate change, it has been suggested that past events (like the 2005 delay; Barth et al. 2007) can be used windows to the future. Based on observations from 2005, changes in the timing of front development could be a factor in catastrophic recruitment failures across entire ecosystems. However, more research is needed to identify how frontal development is linked to observed recruitment failures.

Connectivity among marine populations is a fundamental component of coastal ecosystem structure and dynamics, conservation theory, and fisheries management (Cowen et al. 2006; Gouhier et al. 2010). The influence of fronts on recruitment provides unique insights into potential connectivity patterns. A front near a particular habitat will accumulate larvae from nearby (Fig. 13a) and from far away (Fig. 13b). Both situations have different effects on connectivity depending on the spatiotemporal dynamics of the front, on the presence of a front at larval release, and on species-specific larval behaviors. Our results, however, do not allow determination of whether particular fronts act as barriers to distant dispersers, as accumulators, or even as locally retentive features.

A recent comparison of genetic structure of 15 rockfish species shows much higher levels of genetic differentiation along the California coast in OYB rockfish than KGB rockfish (Sivasundar and Palumbi 2010). Both groups show a positive association of fronts and settlement, suggesting

that for KGB rockfish, fronts are accumulating, whereas for OYB rockfish, fronts are barriers. At this time, available geographic genetic comparisons do not coincide with front locations. Therefore, careful genetic tests of the accumulation and barrier models are needed. It is important to note that genetic tests estimate connectivity at evolutionary time scales, and assignment tests will likely be needed to accurately overcome potential discrepancies between demographic and evolutionary connectivity patterns.

Ocean circulation models coupled with particle tracking and general larval behaviors have been widely used to estimate connectivity patterns for many marine species (Cowen et al. 2006; Cowen and Sponaugle 2009; Galindo et al. 2010). However, ocean circulation models that operate at scales relevant to connectivity studies at the present time often do not resolve the spatiotemporal dynamics of fronts, especially near the coast. Our results suggest that developing parameterizations for sub-mesoscale dynamics, in particular coastal fronts, will be an important step forward in our ability to quantify connectivity in marine ecosystems.

We found that front probability is an important predictor of recruitment of multiple taxa across a large marine ecosystem. These patterns are likely driven by a range of biophysical interactions ranging from passive accumulation to active behavioral responses, increased growth, or enhanced survival. The potential for increased survival and growth, and reduced dispersal at fronts, combined with spatiotemporal predictability of fronts may also explain timing and location of spawning aggregations near shelf-break fronts (Munk et al. 1995; Taylor et al. 2006). These regions also experience increased ecological resilience due to increased recruitment across a range of taxa from community builders (kelps, corals, barnacles, mussels) to top predators (Jones et al 2009; Underwood et al 2009). In addition, this predictability makes regions of high front probability particularly amenable to marine conservation and spatial planning efforts (Etnoyer et al. 2004; Sagarminaga and Arrizabalaga 2010). Finally, developing an understanding of how climate change will alter not only the physical dynamics of fronts, but also the biological interactions at fronts, will be an important avenue of future research (Ferrari 2011).

Acknowledgments

We thank D. Foley at the NOAA Pacific Fisheries Environmental Lab, Data Imaging, Inc. and the NSF-GLOBEC North Pacific Program at Oregon State University for data, and R. K. Cowen, L. Crowder, M. M. Foley, T. Gouhier, M. Wright, and two anonymous reviewers for comments and insights. This is contribution 408 from the Partnership for Interdisciplinary Studies of Coastal Oceans, funded primarily by the David and Lucille Packard and the Gordon and Betty Moore Foundations. C.B.W. was also supported by the Center for Ocean Solutions at Stanford University and the National Science Foundation Ocean Program grant 0824972 during this work.

References

Ainley, D. G., and others. 2009. Association of predators and prey at frontal features in the California Current: Competition, facilitation, and co-occurence. Mar. Ecol. Prog. Ser. **389:** 271–294, doi:10.3354/meps08153

Akaike, H. 1974. A new look at the statistical model identification. IEEE Trans. Automat. Control **19:** 716–723, doi:10.1109/TAC.1974.1100705

Baltz, K. 2009. Cruise report, NOAA Ship David Starr Jordan DS-08-03, May 4–June 18, 2008: Rockfish recruitment assessment [Internet]. NOAA Technical Report. Available from http://swfsc.noaa.gov/publications/FED/01013.pdf.

Barth, J. A., and others. 2007. Delayed upwelling alters nearshore coastal ocean ecosystems in the northern California current. Proc. Natl. Acad. Sci. USA **104:** 3719–3724, doi:10.1073/pnas.0700462104

Belkin, I. M., P. Cornillon, and K. Sherman. 2009. Fronts in large marine ecosystems. Prog. Oceanogr. **81:** 223–236, doi:10.1016/j.pocean.2009.04.015

———, and J. E. O. Reilly. 2009. An algorithm for oceanic front detection in chlorophyll and SST satellite imagery. J. Mar. Syst. **78:** 319–326, doi:10.1016/j.jmarsys.2008.11.018

Bjorkstedt, E. P., L. K. Rosenfeld, B. A. Grantham, Y. Shkedy, and J. Roughgarden. 2002. Distributions of larval rockfish *Sebastes* spp. across nearshore fronts in an upwelling region. Mar. Ecol. Prog. Ser. **242:** 215–228, doi:10.3354/meps242215

Breaker, L. C., T. P. Mavor, and W. W. Broenkow. 2005. Mapping and monitoring large-scale ocean fronts off the California coast using imagery from GOES-10 geostationary satellite. Publication T-056. California Sea Grant College Program, Univ. California.

Broitman, B. R., and others. 2008. Spatial and temporal patterns of intertidal invertebrate recruitment along the west coast of the United States. Ecol. Monogr. **78:** 408–421, doi:10.1890/06-1805.1

Brown, S. K., and J. Roughgarden. 1985. Growth, morphology, and laboratory culture of larvae of *Balanus glandula* (Cirripedia: Thoracica). J. Crustac. Biol. **5:** 574–590, doi:10.2307/1548236

Caselle, J. E., M. H. Carr, D. P. Malone, J. R. Wilson, and D. E. Wendt. 2010*a*. Can we predict interannual and regional variation in delivery of pelagic juveniles to nearshore populations of rockfishes (genus *Sebastes*) using simple proxies of ocean conditions? CalCOFI Rep. **51:** 1–16.

———, B. P. Kinlan, and R. R. Warner. 2010*b*. Temporal and spatial scales of influence on near-shore fish recruitment in the Southern California Bight. Bull. Mar. Sci. **86:** 355–385.

Castelao, R. M., T. P. Mavor, J. A. Barth, and L. C. Breaker. 2006. Sea-surface temperature fronts in the California Current System from geostationary satellite observations. J. Geophys. Res. Oceans **111:** C09026, doi:10.1029/2006JC003541

Cayula, J.-F., and P. Cornillon. 1992. Edge detection algorithm for SST images. J. Atmos. Ocean. Technol. **9:** 67–80, doi:10.1175/1520-0426(1992)009<0067:EDAFSI>2.0.CO;2

Connolly, S. R., B. A. Menge, and J. Roughgarden. 2001. A latitudinal gradient in recruitment of intertidal invertebrates in the northeast Pacific Ocean. Ecology **82:** 1799–1813, doi:10.1890/0012-9658(2001)082[1799:ALGIRO]2.0.CO;2

Cowen, R. K., C. B. Paris, and A. Srinivasan. 2006. Scaling of connectivity in marine populations. Science **311:** 522–527, doi:10.1126/science.1122039

———, and S. Sponaugle. 2009. Larval dispersal and marine population connectivity. Annu. Rev. Mar. Sci. **1:** 442–466. doi:10.1146/annurev.marine.010908.163757

Etnoyer, P., D. Canny, B. Mate, and L. Morgan. 2004. Persistent pelagic habitats in the Baja California to Bering Sea (B2B) ecoregion. Oceanography **17:** 90–101.

Ferrari, R. 2011. A frontal challenge for climate models. Science **332:** 316, doi:10.1126/science.1203632

Galindo, H. M., A. S. Pfeiffer-Hebert, M. A. Mcmanus, Y. Chao, F. Chai, and S. R. Palumbi. 2010. Seascape genetics along a steep cline: Using genetic patterns to test predictions of marine larval dispersal. Mol. Ecol. **19:** 3692–3707, doi:10.1111/j.1365-294X.2010.04694.x

Genin, A. 2004. Biophysical coupling in the formation of zooplankton and fish aggregations over abrupt topographies. J. Mar. Syst. **50:** 3–20, doi:10.1016/j.jmarsys.2003.10.008

Gouhier, T. C., F. Guichard, and B. A. Menge. 2010. Ecological processes can synchronize marine population dynamics over continental scales. Proc. Natl. Acad. Sci. USA **107:** 8281–8286, doi:10.1073/pnas.0914588107

Graham, W. M., and J. L. Largier. 1997. Upwelling shadows as nearshore retention sites: The example of northern Monterey Bay. Cont. Shelf Res. **17:** 509–532, doi:10.1016/S0278-4343(96)00045-3

Jones, G. P., and others. 2009. Larval retention and connectivity among populations of corals and reef fishes: History, advances and challenges. Coral Reefs **28:** 307–325, doi:10.1007/s00338-009-0469-9

Landaeta, M. F., and L. R. Castro. 2006. Larval distribution and growth of the rockfish, *Sebastes capensis* (Sebastidae, Pisces), in the fjords of southern Chile. ICES J. Mar. Sci. **63:** 714–724, doi:10.1016/j.icesjms.2006.01.002

Leslie, H. M., E. N. Breck, F. Chan, B. A. Menge, and J. Lubchenco. 2005. Barnacle reproductive hotspots linked to nearshore ocean conditions. Proc. Natl. Acad. Sci. USA **102:** 10534–10539, doi:10.1073/pnas.0503874102

Mace, A. J., and S. G. Morgan. 2006. Biological and physical coupling in the lee of a small headland: Contrasting transport mechanisms for crab larvae in an upwelling region. Mar. Ecol. Prog. Ser. **324:** 185–196, doi:10.3354/meps324185

Mcculloch, A., and A. L. Shanks. 2003. Topographically generated fronts, very nearshore oceanography and the distribution and settlement of mussel larvae and barnacle cyprids. J. Plankton Res. **25:** 1427–1439, doi:10.1093/plankt/fbg098

Mitarai, S., D. A. Siegel, and K. B. Winters. 2008. A numerical study of stochastic larval settlement in the California Current system. J. Mar. Syst. **69:** 295–309, doi:10.1016/j.jmarsys.2006.02.017

Moffitt, E. A., J. W. White, and L. W. Botsford. 2011. The utility and limitations of size and spacing guidelines for designing marine protected area (MPA) networks. Biol. Conserv. **144:** 306–318, doi:10.1016/j.biocon.2010.09.008

Morgan, S. G., J. L. Fisher, and J. Largier. 2011. Larval retention, entrainment, and accumulation in the lee of a small headland. Limnol. Oceanogr. **56:** 161–178, doi:10.4319/lo.2011.56.1.0161

Munk, P., P. O. Larsson, D. Danielsen, and E. Moksness. 1995. Larval and small juvenile cod (*Gadhus morhua*) concentrated in the highly productive area of a shelf break front. Mar. Ecol. Prog. Ser. **125:** 21–30, doi:10.3354/meps125021

Pierce, S. D., J. A. Barth, R. E. Thomas, and G. W. Fleischer. 2006. Anomalously warm July 2005 in the northern California Current: Historical context and the significance of cumulative wind stress. Geophys. Res. Lett. **33:** L22S04, doi:10.1029/2006GL027149

Pineda, J. 1999. Circulation and larval distribution in internal tidal bore warm fronts. Limnol. Oceanogr. **44:** 1400–1414, doi:10.4319/lo.1999.44.6.1400

Queiroga, H., C. Silva, J. C. Sorbe, and F. Morgado. 2005. Composition and distribution of zooplankton across an upwelling front on the northern Portuguese coast during summer. Hydrobiologia **545:** 195–207, doi:10.1007/s10750-005-2675-y

Roughgarden, J., J. T. Pennington, D. Stoner, S. Alexander, and K. Miller. 1991. Collisions of upwelling fronts with the intertidal zone: The cause of recruitment pulses in barnacle populations of central California. Acta Oecol. **12:** 35–51.

Sagarminaga, Y., and H. Arrizabalaga. 2010. Spatio-temporal distribution of albacore (*Thunnus alalunga*) catches in the northeastern Atlantic: Relationship with the thermal environment. Fish. Oceanogr. **19:** 121–134, doi:10.1111/j.1365-2419.2010.00532.x

Shanks, A. L., A. Mcculloch, and J. Miller. 2003. Topographically generated fronts, very nearshore oceanography and the distribution of larval invertebrates and holoplankters. J. Plankton Res. **25:** 1251–1277, doi:10.1093/plankt/fbg090

Sivasundar, A., and S. R. Palumbi. 2010. Life history, ecology and the biogeography of strong genetic breaks among 15 species of Pacific rockfish, *Sebastes*. Mar. Biol. **157:** 1433–1452, doi:10.1007/s00227-010-1419-3

Strathmann, R. R. 1985. Feeding and non-feeding larval development and life-history evolution in marine invertebrates. Annu. Rev. Ecol. Syst. **16:** 339–361, doi:10.1146/annurev.es.16.110185.002011

Taylor, J. C., D. B. Eggleston, and P. S. Rand. 2006. Nassau grouper (*Epinephelus striatus*) spawning aggregations: Hydroacoustic surveys and geostatistical analysis. NOAA Prof. Pap. NMFS **5:** 18–25.

Traganza, E. D., D. G. Redalje, and R. W. Garwood. 1987. Chemical flux, mixed layer entrainment, and phytoplankton blooms at upwelling fronts in the California coastal zone. Cont. Shelf Res. **7:** 89–105, doi:10.1016/0278-4343(87)90066-5

Underwood, J. N., L. D. Smith, M. J. H. Van Oppen, and J. P. Gilmour. 2009. Ecologically relevant dispersal of corals on isolated reefs: Implications for managing resilience. Ecol. Appl. **19:** 18–29, doi:10.1890/07-1461.1

Wing, S. R., J. Largier, L. W. Botsford, and J. F. Quinn. 1995. Settlement and transport of benthic invertebrates in an intermittent upwelling region. Limnol. Oceanogr. **40:** 316–329, doi:10.4319/lo.1995.40.2.0316

Wolanski, E., and W. M. Hamner. 1988. Topographically-controlled fronts in the ocean and their biological influence. Science **241:** 177–181, doi:10.1126/science.241.4862.177

Woodson, C. B., and M. A. McManus. 2007. Foraging behavior can influence dispersal of marine organisms. Limnol. Oceanogr. **52:** 2701–2709, doi:10.4319/lo.2007.52.6.2701

Associate editor: Craig L. Stevens

Received: 28 February 2011
Accepted: 16 November 2011
Amended: 28 November 2011